

Supplementary data Hexaferrocenylbenzene

Yong Yu, Andrew D. Bond, Philip W. Leonard, Ulrich J. Lorenz, Tatiana V. Timofeeva, K. Peter C. Vollhardt, Glenn D. Whitener and Andrey A. Yakovenko

General. All reactions and chromatographic separations were performed under a nitrogen atmosphere in oven-dried glassware. Materials obtained commercially were used without further purification. Solvents were dried by distillation over the corresponding drying agents and degassed by nitrogen purge (15 min) prior to use.

Melting points were taken in open capillary tubes, using a Thomas Hoover Unimelt apparatus, and are uncorrected. Mass spectral measurements and elemental analyses were performed by the Micro Mass Facility of the University of California at Berkeley. NMR spectra were recorded on Bruker DRX-500, AVB-400, AVQ-400, and AV-300 spectrometers, with working frequencies (for ^1H nuclei) of 500, 400, 400, and 300 MHz, respectively. ^{13}C -NMR spectra were recorded with simultaneous decoupling of ^1H nuclei. ^1H -NMR chemical shifts are reported in ppm units relative to the residual signal of the solvent. IR measurements were performed on Perkin Elmer System 2000 FT-IR spectrometer. Column chromatography was carried out on silica gel 60, 32–63 mesh. Analytical TLC was performed on Merck aluminum-backed silica gel plates.

Ferrocenylation of hexaiodobenzene. Under N_2 , BuLi (53.1 mL, 85.0 mmol, 1.6 M in hexane) was added dropwise to FcI (26.5 g, 85.0 mmol) in ether (300 mL) at $-78\text{ }^\circ\text{C}$ within 8 min to form a yellow suspension, which was stirred for 45 min. The reaction mixture was stirred at rt for 30 min, hexane (120 mL) added, followed by cooling to $-78\text{ }^\circ\text{C}$ for 10 min, and then filtration to remove the solvent containing BuI. The resulting yellow powder was washed with hexane (3x40 mL) and dried under vacuum (0.1 torr) at rt for 1.5 h. THF was then added (150 mL) at $-78\text{ }^\circ\text{C}$, followed by ZnBr_2 (9.57 g, 42.5 mmol) in THF (80 mL) during 4 min, and the mixture stirred for 10 min, warmed to rt, and stirred for an additional 40 min. In a separate three-necked flask, PhI_6 (5.90 g, 7.08 mmol) and $\text{Pd}_2(\text{dba})_3$ (1.94 g, 2.12 mmol) were stirred in THF (300 mL) at rt for 15 min to give a black suspension. To this mixture at $65\text{ }^\circ\text{C}$ was added the above Fc_2Zn solution dropwise during 50 min, and stirring and heating was continued for 63 h. After cooling to rt, H_2O (2 mL) was added, and the entire blend was filtered through a silica column (4x16

cm), eluting with CH₂Cl₂/EtOAc/hexane = 50/10/3, to provide a red solid on evaporation of the solvents. Chromatography on silica (column size 4x18 cm), eluting with a solvent gradient of CH₂Cl₂/hexane = 1/20 to 5/1, gave a red solution containing **1** and **2**. Renewed chromatography using trichloroethene/hexane/EtOAc = 1/8/0.3 afforded the **2** as an orange-red powder (3.96 g, 56%) and **1** as a yellow-orange powder (334 mg, 4%).

Ferrocenylation of hexabromobenzene. The procedure described above was repeated in an identical manner, but using hexabromobenzene as the substrate, to give, in order of elution **4** (10%) and a mixture containing **1–3** contaminated by other partly ferrocenylated products, including **5** (mass spectral analysis), from which **1** (1%) could be precipitated using CH₂Cl₂. The remainder was resubjected to column chromatography, eluting with petroleum ether/CH₂Cl₂ to separate **2** (4%). From one of the fractions, a crystal of orange **3** could be obtained by slow evaporation of CH₂Cl₂. Attempted HPLC separation (silica, hexanes/CH₂Cl₂) of the supernatant was unsuccessful in generating more material.

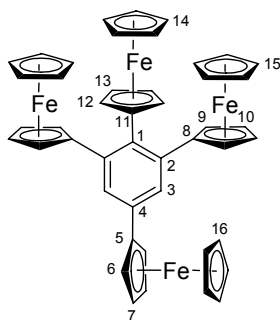
In an attempt to improve on these results, reactions conditions were varied as follows. Ferrocene (6.0 g, 32.3 mmol) was suspended in THF (16 mL) and hexanes (16 mL) at 0 °C. During 25 min, a 1.7 M solution of *tert*-BuLi in pentane (19 mL, 32.3 mmol) was injected and the slurry stirred for another 5 min, before ZnCl₂ (2.20 g, 16.1 mmol) in THF (30 mL) was added. The resulting orange mixture was allowed to warm up to rt, stirred for another 30 min, reduced in volume to 40 mL, and cannulated into a slurry of hexabromobenzene (593 mg, 1.08 mmol), PdCl₂(dppf) (70.2 mg, 0.096 mmol), and Pd₂(dba)₃·CHCl₃ (49.8 mg, 0.048 mmol) in 1,4-dioxane (50 mL). The reaction mixture was then refluxed for 24 h, before another aliquot of Fc₂Zn (prepared as above) was added together with half an aliquot each of both catalysts. The mixture was refluxed for another 48 h. The solvent was removed in vacuo and replaced by Et₂O (100 mL). The resulting suspension was filtered and the insoluble parts taken up in CH₂Cl₂, preadsorbed onto silica, and subjected to column chromatography (petroleum ether/CH₂Cl₂) to give fractions containing (in order of elution) **5** and **1**. The contents of the fractions enriched in **1** were dissolved in CH₂Cl₂, and **1** was precipitated by addition of Et₂O to furnish pure

product (15 mg, 1.2%) as an orange powder. Similar treatment of the fractions enriched in **5** gave pure product (47.0 mg, 5.4%) as an orange-yellow powder.

Spectral data

3: orange crystal. MS-FAB (m/z , %): 1080 (M^+ , 15), 1079 (35), 1078 (50), 1077 (43), 1076 (49), 1075 (13), 1074 (18), 997 (M^+ -Br, 8). This compound was not obtained in sufficient quantity to permit full characterization.

4: orange-red crystals. Mp: 170 °C (decomp.). Anal.: Calc. for $C_{36}H_{28}Br_2Fe_3$: C, 54.87; H, 3.58%. Found: C, 55.0; H 3.87%. HRMS (m/z): Calc. for $C_{36}H_{28}Br_2Fe_3$: 785.8606. Found: 785.8604. 1H NMR (500 MHz, CD_2Cl_2 , δ/ppm): 8.34 (s, 1H), 4.69 (br s, 2H), 4.38 (br s, 2H), 4.31 (s, 5H), 4.18 (br s, 2H), 4.15 (br s, 2H), 4.14 (s, 5H), 4.12 (br s, 2H), 4.08 (s, 5H), 3.98 (br s, 2H). $^{13}C\{^1H\}$ NMR (100 MHz, CD_2Cl_2 , δ/ppm): 140.3, 138.2, 136.9, 134.9 (CH_{arom}), 128.0, 125.3, 89.6 (Cp_{quat}), 88.9 (Cp_{quat}), 87.1 (Cp_{quat}), 73.1, 71.1 (2C), 70.0 (Cp), 69.96 (Cp), 69.85 (Cp), 68.3, 67.7, 67.1. UV/VIS (CH_2Cl_2 , nm/ ϵ): 289 (22600), 361 (5970), 457 (1690).



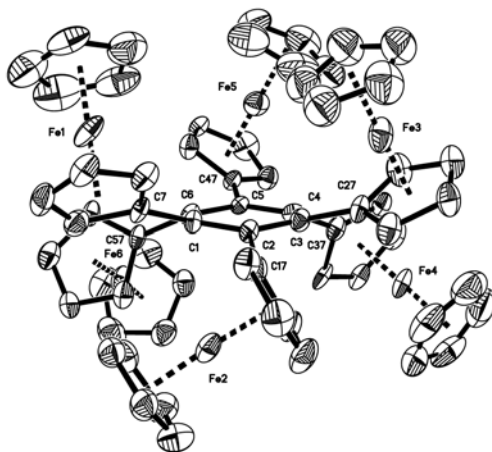
5: orange-yellow powder. Mp: 200 °C (decomp.). Anal.: Calc. for $C_{46}H_{38}Fe_4$: C, 67.86; H, 4.70%. Found: C, 67.79; H, 4.53%. HRMS (m/z): Calc. for $C_{46}H_{38}Fe_4$: 814.0371. Found: 814.0391. 1H NMR (400 MHz, $CDCl_3$, δ/ppm): 8.12 (s, 2H, H3), 4.91 (t, J = 1.8 Hz, 2 H, H12), 4.47 (m, 2 H, H13), 4.46 (m, 4H, H9), 4.30 (m, 4 H, H10), 4.26 (s, 10 H, H15), 4.23 (s, 5 H, H14), 3.96 (t, J = 1.8 Hz, 2 H, H6), 3.93 (t, J = 1.8 Hz, 2 H, H7), 3.66 (s, 5 H, H16). $^{13}C\{^1H\}$ NMR (100 MHz, $CDCl_3$, δ/ppm): 139.1 (C2), 134.3 (C1/4), 134.1(C4/1), 129.0 (C3), 92.4 (C8), 84.3 (C11), 73.5 (C7), 73.3 (C5), 72.2 (C9), 69.7 (C15, C16), 69.6 (C14), 68.9 (C13), 67.0 (C10), 66.5 (C6), 65.6 (C12). IR (KBr, cm^{-1}): 3102, 1404, 1105, 1003, 815.

Details of the X-ray crystallography

1a: $C_{66}H_{54}Fe_6 \cdot C_6H_6$, $M = 1260.3$, $T = 100(2)$ K, crystal size $0.30 \times 0.10 \times 0.02$ mm³, monoclinic, space group $C2/c$, $a = 39.8230(12)$, $b = 11.4629(3)$, $c = 22.8543(6)$ Å, $\alpha = 90$, $\beta = 90.923(1)$, $\gamma = 90^\circ$, $V = 10431.3(5)$ Å³, $Z = 8$, $D_{\text{calc}} = 1.605$ g cm⁻³, $\mu(\text{Mo K}\alpha) = 1.672$ mm⁻¹, 9210 unique reflections, of which 6409 were taken as observed [$I > 2\sigma(I)$], $R1 = 0.041$, $wR2 = 0.104$ (all data), $S = 1.01$.

One residual peak in the electron density (ca 3.8 Å⁻³) lies on the special position (0,0.234,1/4) in the solvent region. This peak lies half-way between two benzene solvent molecules, with H...Q distances of 1.22 Å – it cannot be modeled as any physically reasonable atom. There is likely to be some disorder in this solvent region. Comparison with the structure of **1b** supports this suggestion (see below).

1b: $C_{66}H_{54}Fe_6 \cdot \frac{1}{2}(C_6H_4Cl_2)$, $M = 1255.7$, $T = 220(2)$ K, crystal size $0.14 \times 0.10 \times 0.01$ mm³, monoclinic, space group $I2/a$, $a = 44.218(11)$, $b = 11.535(2)$, $c = 22.898(5)$ Å, $\alpha = 90$, $\beta = 93.960(9)$, $\gamma = 90^\circ$, $V = 11651(4)$ Å³, $Z = 8$, $D_{\text{calc}} = 1.432$ g cm⁻³, $\mu(\text{synchrotron}, \lambda = 0.6850 \text{ Å}) = 1.541$ mm⁻¹, 8218 unique reflections, of which 5820 were taken as observed [$I > 2\sigma(I)$], $R1 = 0.105$, $wR2 = 0.291$ (all data), $S = 1.04$.



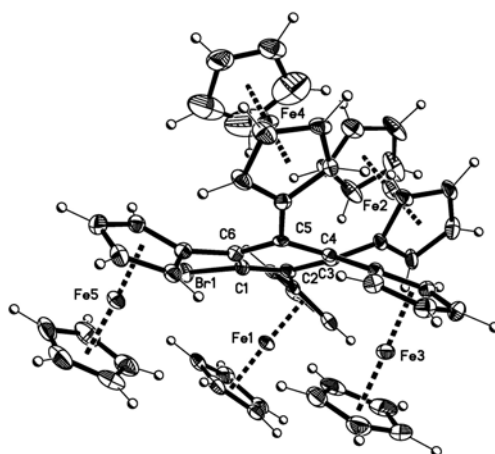
All C atoms are refined with anisotropic displacement parameters, restrained to approximate isotropic behavior (ISOR restraints in *SHELXL*). The dichloromethane molecule (not shown in the diagram above) is included with 50% site occupancy to

provide acceptable displacement parameters. Voids remain within the structure in the solvent region, containing some diffuse residual electron density. It is likely that more solvent molecules are present in this region, but these cannot be satisfactorily resolved.

2: $C_{56}H_{46}Fe_5$, $M = 998.2$, $T = 130(2)$ K, crystal size $0.50 \times 0.20 \times 0.18$ mm³, triclinic, space group $P\bar{1}$, $a = 11.9387(7)$, $b = 12.4181(7)$, $c = 15.7154(9)$ Å, $\alpha = 99.808(1)$, $\beta = 100.205(1)$, $\gamma = 115.062(1)^\circ$, $V = 1996.9(2)$ Å³, $Z = 2$, $D_{\text{calc}} = 1.660$ g cm⁻³, $\mu(\text{Mo K}\alpha) = 1.815$ mm⁻¹, 6443 unique reflections, of which 5410 were taken as observed [$I > 2\sigma(I)$], $R1 = 0.050$, $wR2 = 0.133$ (all data), $S = 1.03$.

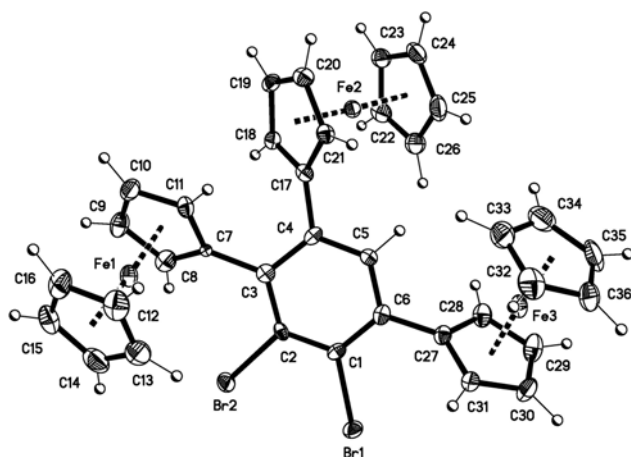
All C atoms are refined with anisotropic displacement parameters, restrained to approximate isotropic behavior (ISOR restraints in *SHELXL*). Residual peaks/holes in the electron density lie in the vicinity of the Fe atoms.

3: $C_{56}H_{45}BrFe_5 \cdot 1.5(C_6H_4Cl_2)$, $M = 1297.6$, $T = 155(2)$ K, crystal size $0.23 \times 0.20 \times 0.17$ mm³, monoclinic, space group $C2/c$, $a = 21.0124(5)$, $b = 12.2354(3)$, $c = 40.4132(8)$ Å, $\alpha = 90$, $\beta = 94.812(1)$, $\gamma = 90^\circ$, $V = 10353.4(4)$ Å³, $Z = 8$, $D_{\text{calc}} = 1.665$ g cm⁻³, $\mu(\text{Mo K}\alpha) = 2.338$ mm⁻¹, 8713 unique reflections, of which 6025 were taken as observed [$I > 2\sigma(I)$], $R1 = 0.053$, $wR2 = 0.127$ (all data), $S = 1.02$.



All C atoms are refined with anisotropic displacement parameters, restrained to approximate isotropic behavior (ISOR restraints in *SHELXL*). Residual peaks/holes in the electron density lie in the vicinity of the Fe atoms.

4: $C_{36}H_{28}Br_2Fe_3 \cdot \frac{1}{2}(CH_2Cl_2)$, $M = 830.4$, $T = 133(2)$ K, crystal size $0.27 \times 0.20 \times 0.11$ mm³, triclinic, space group $P\bar{1}$, $a = 10.9153(3)$, $b = 11.6153(3)$, $c = 13.5364(4)$ Å, $\alpha = 98.956(1)$, $\beta = 98.956(1)$, $\gamma = 98.170(1)^\circ$, $V = 1508.32(7)$ Å³, $Z = 2$, $D_{calc} = 1.828$ g cm⁻³, $\mu(Mo K\alpha) = 4.188$ mm⁻¹, 4826 unique reflections, of which 4110 were taken as observed [$I > 2\sigma(I)$], $R1 = 0.043$, $wR2 = 0.114$ (all data), $S = 1.04$.



All C atoms are refined with anisotropic displacement parameters, restrained to approximate isotropic behavior (ISOR restraints in *SHELXL*).

Geometrical parameters in **1a**, **1b**, **2**, **3** and **4**

- Distances (Å) and angles (°) in the benzene ring

	1a	1b	2	3	4
C1–C2	1.413(6)	1.416(14)	1.426(6)	1.398(7)	1.396(6)
C2–C3	1.431(5)	1.437(14)	1.434(6)	1.422(7)	1.431(6)
C3–C4	1.409(5)	1.393(13)	1.428(6)	1.422(7)	1.439(6)
C4–C5	1.431(5)	1.434(13)	1.417(6)	1.415(7)	1.392(6)
C5–C6	1.415(5)	1.438(14)	1.392(6)	1.416(7)	1.378(6)
C6–C1	1.419(5)	1.416(14)	1.392(6)	1.413(7)	1.396(6)

C1–C2–C3	119.1(4)	118.7(8)	117.4(4)	116.9(5)	123.0(4)
C2–C3–C4	119.7(4)	119.8(9)	118.5(4)	118.6(5)	113.9(3)
C3–C4–C5	119.8(4)	121.1(8)	117.7(4)	119.8(5)	121.2(4)
C4–C5–C6	118.7(4)	118.0(8)	118.4(4)	118.0(5)	123.4(4)
C5–C6–C1	120.0(4)	119.8(9)	122.7(4)	117.4(5)	117.1(4)
C6–C1–C2	119.8(4)	120.3(9)	119.0(4)	124.4(5)	121.0(4)

• Torsion angles (°) in the benzene ring

	1a	1b	2	3	4
C1–C2–C3–C4	–13.7(6)	–13.0(14)	24.5(5)	12.0(7)	6.7(6)
C2–C3–C4–C5	14.0(6)	12.4(15)	–29.4(6)	–25.2(7)	–5.2(6)
C3–C4–C5–C6	–14.2(6)	–11.5(14)	14.6(6)	26.2(7)	0.2(7)
C4–C5–C6–C1	14.2(6)	11.5(14)	4.9(6)	–14.1(7)	3.6(7)
C5–C6–C1–C2	–14.2(6)	–12.8(15)	–9.7(6)	1.6(8)	–2.1(7)
C6–C1–C2–C3	13.7(6)	13.3(15)	–5.2(6)	–0.6(8)	–3.2(7)

• Fe···Cp(centroid) distances (Å) and angles (°)

[Centroid C100 refers to ring C7–C11, C101 to ring C12–C16, C102 to ring C17–C21, *etc.*]

	1a	1b	2	3	4
Fe1–C100	1.644	1.642	1.670	1.655	1.656
Fe1–C101	1.647	1.656	1.654	1.656	1.664
Fe2–C102	1.655	1.669	1.657	1.652	1.654
Fe2–C103	1.656	1.659	1.650	1.650	1.660
Fe3–C104	1.640	1.650	1.663	1.651	1.651
Fe3–C105	1.644	1.650	1.651	1.669	1.656
Fe4–C106	1.653	1.644	1.649	1.636	
Fe4–C107	1.653	1.654	1.656	1.649	
Fe5–C108	1.650	1.633	1.657	1.652	
Fe5–C109	1.654	1.650	1.655	1.649	
Fe6–C110	1.651	1.646			
Fe6–C111	1.653	1.666			
C100–Fe1–C101	177.7	177.5	174.1	174.5	176.7
C102–Fe2–C103	176.0	176.9	175.2	171.5	178.3

C104–Fe3–C105	177.9	178.5	178.5	169.3	177.2
C106–Fe4–C107	175.8	175.7	179.0	169.6	
C108–Fe5–C109	179.2	178.2	177.6	172.0	
C110–Fe6–C111	176.7	176.4			

- C(arom)–C(quat) distances (Å), C(arom)–C(quat)⋯Cp(centroid) angles (°)
 [Centroid C100 refers to ring C7–C11, C101 to ring C12–C16, C102 to ring C17–C21, etc.]

	1a	1b	2	3	4
C1*–C7	1.498(5)	1.506(13)	1.492(6)	1.500(7)	1.508(2)
C2–C17	1.507(6)	1.495(14)	1.478(6)	1.506(7)	1.487(6)
C3–C27	1.496(5)	1.498(14)	1.498(6)	1.499(7)	1.497(6)
C4–C37	1.511(5)	1.514(8)	1.496(6)	1.500(7)	
C5–C47	1.496(5)	1.495(13)	1.480(6)		
C6–C57	1.510(5)	1.504(14)			
C1*–C7⋯C100	172.7	173.4	172.4	173.1	176.7
C2–C17⋯C102	168.2	168.2	175.9	171.5	178.3
C3–C27⋯C104	173.4	173.1	169.6	169.3	177.2
C4–C37⋯C106	166.0	166.3	172.5	169.6	
C5–C47⋯C108	173.7	172.9	178.3	172.0	
C6–C57⋯C110	166.3	166.4			

* Labeling refers specifically to **1a**, **1b** and **2**. Labels for the first C atom is changed appropriately for **3** and **4** (see ellipsoid plots).

- C(arom)–C(arom)–C(quat)–C torsions (°)

	1a	1b	2	3	4
C6*–C1*–C7–C11	37.4(7)	39.5(17)	86.2(6)	52.9(8)	–44.5(7)
C1–C2–C17–C18	–75.8(6)	–75.5(17)	31.1(7)	–54.3(9)	–47.4(6)
C2–C3–C27–C31	28.3(7)	29.1(18)	–28.2(7)	3.2(8)	–57.2(6)
C3–C4–C37–C41	–84.2(6)	–85.2(16)	15.8(6)	19.3(7)	
C4–C5–C47–C51	26.6(6)	26.5(17)	37.6(7)	–45.3(7)	
C5–C6–C57–C58	–85.8(6)	–89.0(14)			

* Labeling refers specifically to **1a**, **1b** and **2**. Labels for the first two C atoms are changed appropriately for **3** and **4** (see ellipsoid plots).

- C(quat)–C(arom)–C(arom)–C(quat) torsions (°)

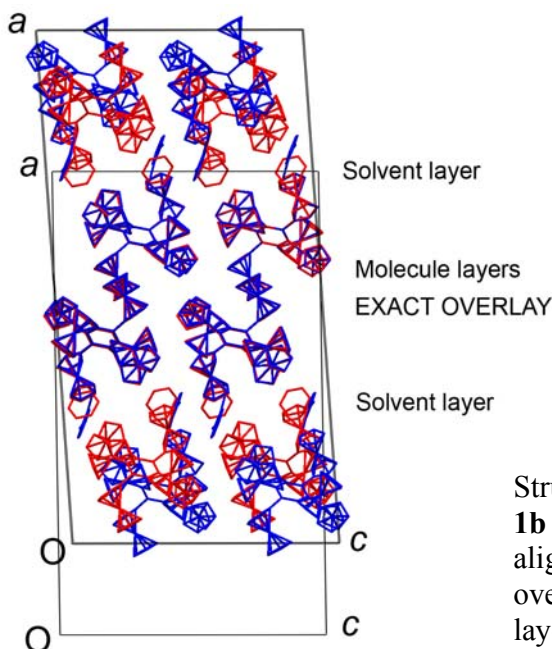
	1a	1b	2	3	4
C7–C1*–C2*–C17	39.1(5)	41.1(14)	–14.0(6)	28.8(7)	–3.8(6)

C17–C2–C3–C27	–37.5(5)	–38.0(14)	35.6(6)	–44.3(6)
C27–C3–C4–C37	38.9(6)	37.5(15)	–47.9(5)	47.0(6)
C37–C4–C5–C47	–37.8(5)	–37.5(13)	26.5(6)	–29.3(7)
C47–C5–C6–C57	40.5(6)	43.1(13)		
C57–C6–C1–C7	–39.5(5)	–42.7(13)		

* Labeling refers specifically to **1a**, **1b** and **2**. Labels for the central two C atoms are changed appropriately for **3** and **4** (see ellipsoid plots).

Comparison of structure **1a** and **1b**

The structures of **1a** and **1b** resemble each other closely. The molecular structures are essentially indistinguishable: the 42 non-H atoms of the central core (*i.e.* excluding the outer Cp rings which display small rotational differences) can be overlaid with an r.m.s. deviation of only 0.04 Å. In both structures, the molecules form layers parallel to the (100) planes of the unit cell. These layers are also essentially indistinguishable, reflected in the closely comparable *b* and *c* lattice parameters. Along the *a* direction, the structures are arranged: molecule layer—molecule layer—solvent layer—molecule layer—molecule layer—solvent layer, etc. The arrangement of the *pairs* of molecule layers is indistinguishable in both structures.



The distinction between the two structures lies in the solvent region. In **1a**, adjacent pairs of layers are offset along *b* by half of the lattice parameter (giving rise to the *C* centering), while in **1b** they are offset along both *b* and *c* by half of each lattice parameter (giving rise to the *I* centering).

The layered arrangement in the structures accounts for the formation of thin plates. This solvent region is likely to be disordered to some extent. Any loss of solvent will lead to irregularities in the layered arrangement. This accounts for the diffuse nature of the structure in **1b** (for which the data are of low precision) and the residual electron density in this region for **1a**.

Voltammetry

Osteryoung Square Wave Voltammetry (OSWV) and Cyclic Voltammetry (CV) were performed on a 10mg sample of hexaferrocenylbenzene in 10ml of a 1.0 M NBu₄PF₆ dichloromethane solution. Data were recorded using a three electrode cell with a glassy carbon working electrode, a platinum wire auxiliary electrode, and a silver wire reference electrode connected to a BAS 100b electroanalyzer, all values are corrected to [Cp₂Fe]/[Cp₂Fe]⁺.

From the OSWV data, three separate peaks with E_{1/2} values of -162.8, -32.3, and 222.4mV could be measured with peak currents of 13.8, 15.8, and 20.9, respectively. Peak sizes and shapes are most consistent with a one electron oxidation, followed by a two electron, and, finally, a three electron wave.

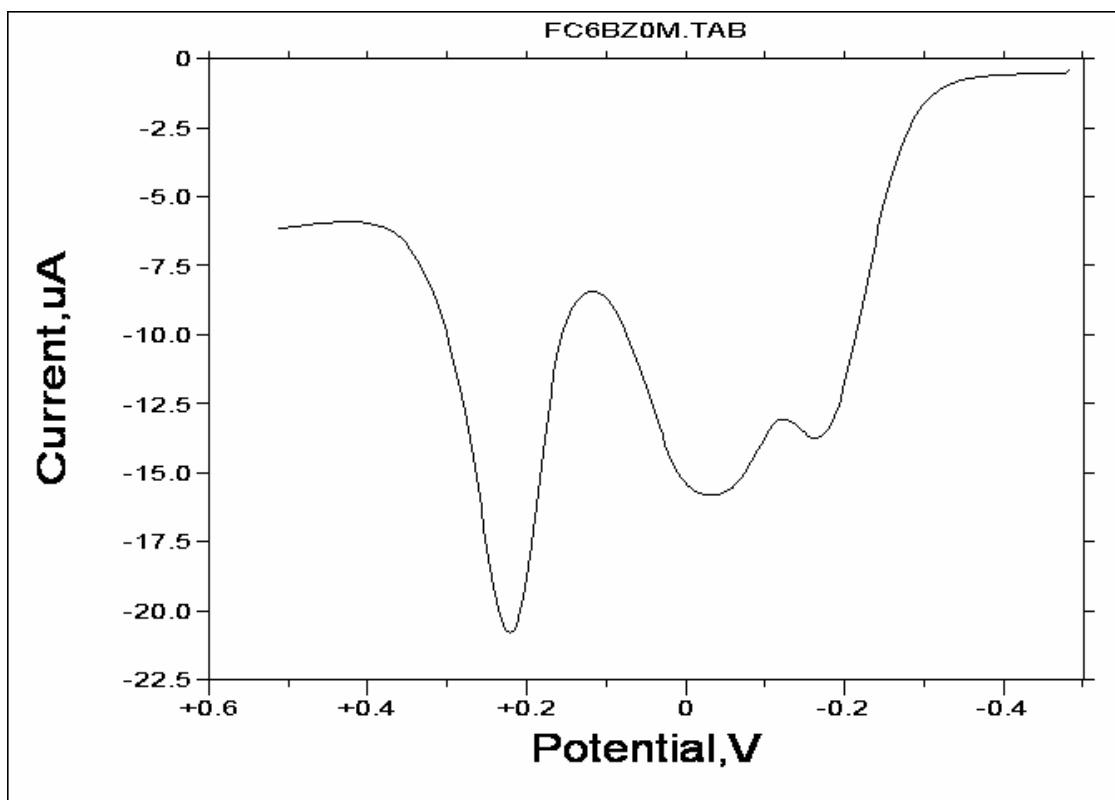


Figure 1 Osteryoung Square Wave Voltammetry Plotted vs. Fc/Fc+
Experimental conditions: Initial E (mV) = 0, Final E (mV) = 1000, Step E (mV) = 4,
S.W. Amplitude (mV) = 25, Frequency (Hz) = 15

Technique	OSWV [mV]		CV [mV]
		E_{pc1}	-211
		E_{pa1}	-136.9
		$E_{pa} - E_{pc}$	74.1
$E_{1/21}$ (ip [μ A])	-162.8 (13.8)	$E_{1/21}$	-174
		E_{pc2}	-104.9
		E_{pa2}	36.5
		$E_{pa} - E_{pc}$	141.4
$E_{1/22}$ (ip [μ A])	-32.2 (15.8)	$E_{1/22}$ [mV]	-34.2
		E_{pc3}	23
		E_{pa3}	NA
		$E_{pa} - E_{pc}$	NA
$E_{1/23}$ (ip [μ A])	222.4 (20.9)	$E_{1/23}$ [mV]	NA

Table 1 Electrochemical data Values are vs. Fc/Fc+

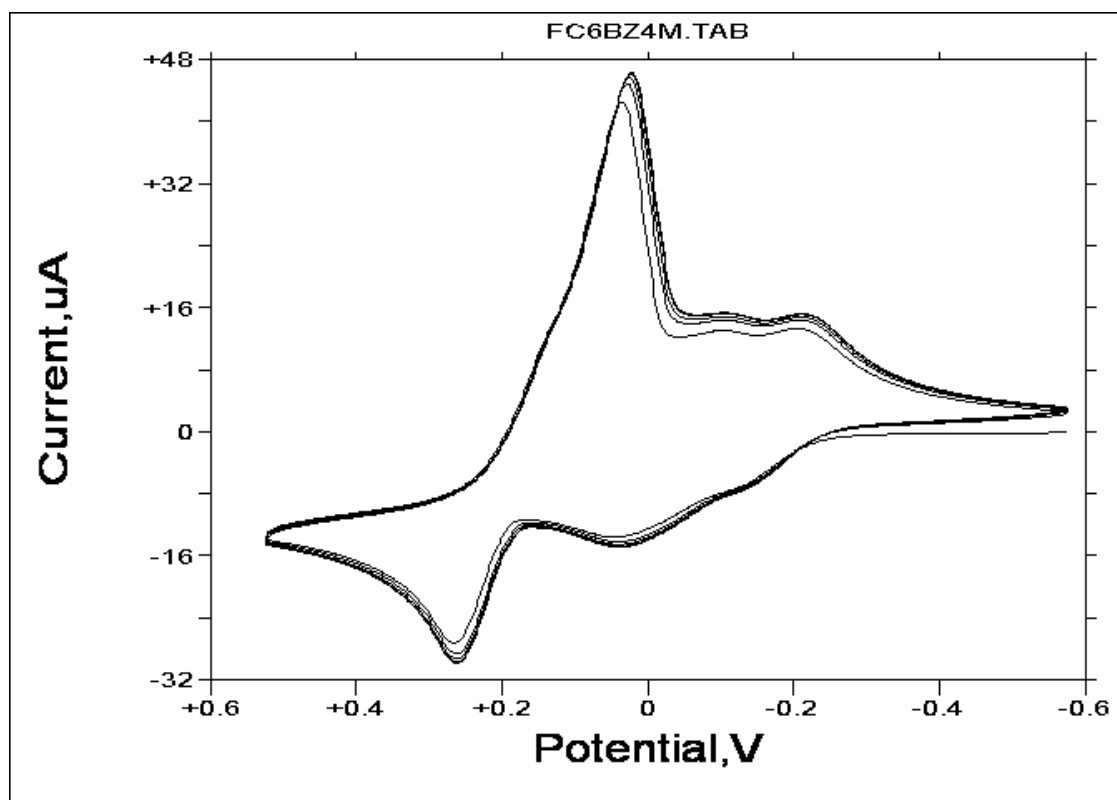


Figure 2 Cyclic voltammetry Plotted vs. Fc/Fc+
 Experimental conditions: Initial E (mV) = -100, High E (mV) = 1000, Low E (mV) = -100,
 Initial = Positive, V (mV/sec) = 100

Cyclic voltammetry demonstrated three reversible redox couples, which remained unchanged qualitatively after five full cycles, regardless of scan rate. The disproportionate cathodic peak current in wave 3 is believed to originate from precipitation of the hexacation on the surface of the electrode. None of the redox waves show stringent Nernstian behavior, as demonstrated by the large $E_{pa}-E_{pc}$ values, although the ratio i_p/\sqrt{v} is relatively constant with respect to the first two redox couples for scan rates between 10 and 200 mV/s. The first two waves can be isolated from the third by choosing a narrower sweep width, but their behavior is unchanged.

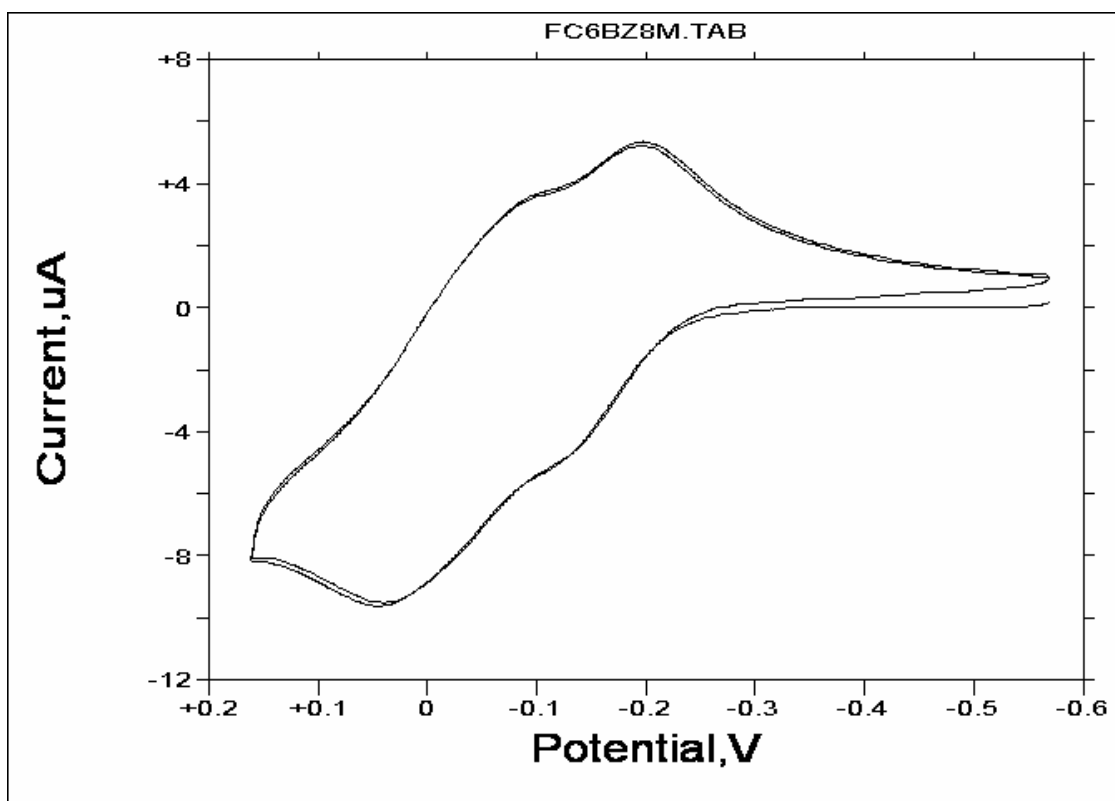


Figure 3 Cyclic voltammetry of the first and second waves Plotted vs. Fc/Fc+
Exp. Conditions: Initial E (mV) = -100, High E (mV) = 630, Low E (mV) = -100,
Initial = Positive, V (mV/sec) = 50